ELSEVIER

Polymer 41 (2000) 2677–2690

polymer

Secondary transitions of aryl–aliphatic polyamides I. Broadband dielectric investigation

F. Beaume[a], F. Lauprêtre[a,*], L. Monnerie[a], A. Maxwell[b], G.R. Davies[b]

[a]*Laboratoire de Physicochimie Structurale et Macromoléculaire associé au CNRS, Ecole Supérieure de Physique et Chimie Industrielles de la Ville de Paris, 75231 Paris Cedex 05, France*

[b]*Interdisciplinary Research Center in Polymer Science and Technology, The University of Leeds, Leeds LS2 9JT, UK*

Received 4 May 1999; accepted 9 June 1999

Abstract

Dielectric relaxation measurements were performed on two series of aryl–aliphatic copolyamides. The repeat unit of the first series was made of 1 or 1.8 lactam-12 sequences, a tere- or iso-phthalic moiety, and a 3,3′-dimethyldicyclohexylmethane unit in regular order. The second series was obtained from condensation of terephthalic acid onto 1,5-diamino-2-methylpentane. The dielectric relaxation measurements demonstrated the existence of several secondary relaxations. The comparison of the results obtained from the two series of samples permitted the assignment of γ, β and ω relaxations, observed in the first series of compounds, to motions of non-conjugated C=O groups, C=O groups located between a phenyl ring and a flexible lactam-12 or methylpentane sequence, and C=O groups situated between a phenyl ring and a rigid cycloaliphatic moiety, respectively.

Keywords: Aryl–aliphatic copolyamides; Dielectric relaxation; Secondary transitions

1. Introduction

Aryl–aliphatic polyamides are industrial technical polymers whose uses as transparent plastics require higher performances than those of polycarbonate and polymethylmethacrylate in terms of temperature behavior or resistance to solvents and stress cracking. The latter properties are usually met with in the polyamides. The temperature behavior of polyamides, which is largely related to the value of the glass transition temperature, can be significantly improved by inserting some aromatic units in the chain sequence. The transparency of materials necessitates a completely amorphous structure that is seldom encountered in either aliphatic or aromatic polyamides themselves. However, crystallinity can be avoided by using not only *para*-substituted phenyl rings, but also *meta*-substituted phenyl rings that decrease the chain regularity. Several aryl–aliphatic polyamides, which are based on these simple ideas, were developed. Dynamit Nobel Trogamid®, E.M.S. Grilamid®, DuPont de Nemours Zytel® or Elf-Atochem Cristamid® are typical examples.

The present work aims to investigate the relationships that may exist between the chemical structure of aryl–aliphatic polyamides and some of their macroscopic properties. The chemical structure is responsible for some static characteristics such as the nature of interactions that take place between atoms, the molecular cohesion, and chain packing. It defines a reference state of the material that can be eventually observed at very low temperatures. However, on increasing the temperature, these initial properties become considerably modified by molecular motions. As with static properties, the local chain dynamics is also largely controlled by the chemical structure. In the present work, we will focus on the investigation of the local motions that may occur in the glassy state of some representative aryl–aliphatic polyamides and might take part in secondary transitions. We will first report results obtained by using dielectric relaxation experiments. The dynamic mechanical, ^{13}C and ^{2}H NMR investigation of these polymers will be published in the forthcoming papers of this series [1–3].

The polymers used for this study are the xT_yI_{1-y} copolyamides, whose repeat unit contains, x lactam-12 sequences, y and $1-y$ tere- and iso-phthalic moieties, respectively, and a 3,3′-dimethyldicyclohexylmethane unit

* Corresponding author. Laboratoire de Recherche sur les Polymères, CNRS, 2 à 8 rue Henri Dunant, 94320 Thiais, France. Tel.: + 33-1-4978-1286, fax: + 33-1-4978-1208.

E-mail address: laupretre@glvt-cnrs.fr (F. Lauprêtre)

0032-3861/00/$ - see front matter
PII: S0032-3861(99)00437-1

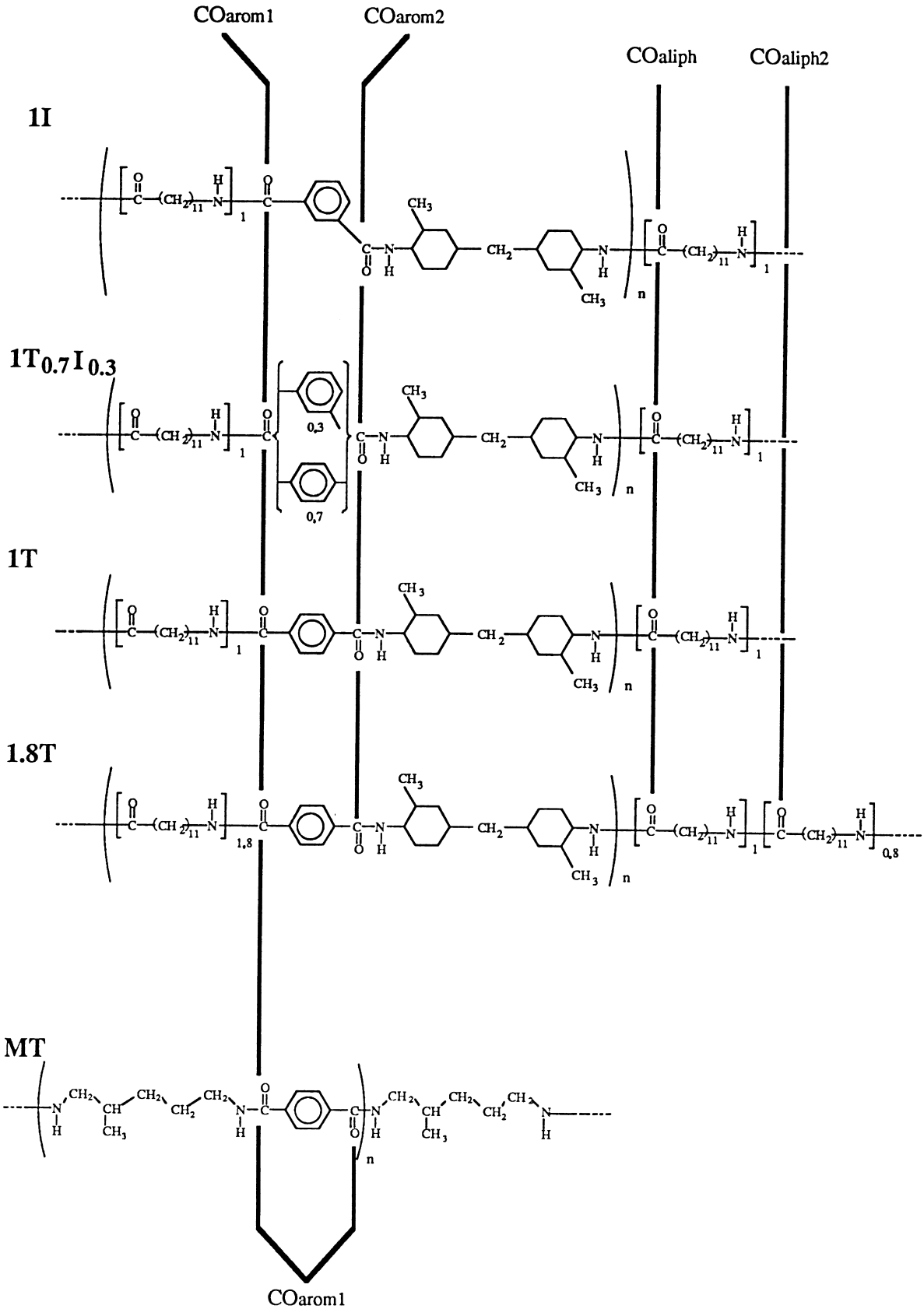

Fig. 1. Chemical formulae of the polyamides under study.

Table 1
Composition in terms of x and y values, molecular weight (in polyamide 12 equivalent), M_w, glass transition temperatures as determined from DSC and amorphous or semicrystalline character of the samples under study

Code name	M_w (g mol^{-1})	x	y	T_g (°C)	Amorphous/crystalline character
1I	19 900	1	0	151	Amorphous
$1T_{0.7}I_{0.3}$	22 400	1	0.7	154	Amorphous
1T	18 600	1	1	157	Low crystallinity
1.8T	31 600	1.8	1	122	Amorphous
MT			1	138	Semicrystalline

in the regular order [4]:

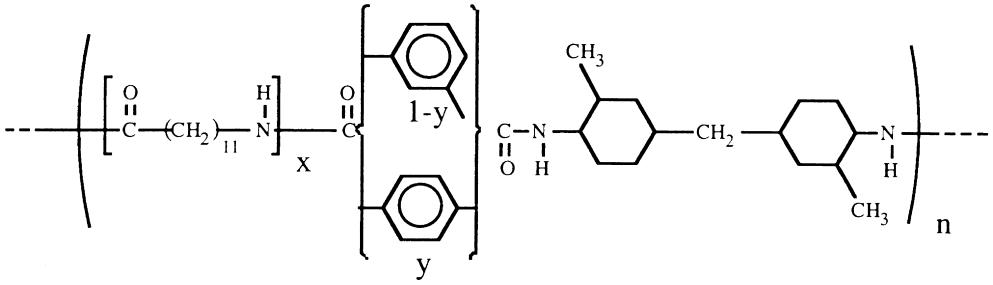

and the following polyamide (MT), obtained from the condensation of terephthalic acid onto 1,5-diamino-2-methylpentane:

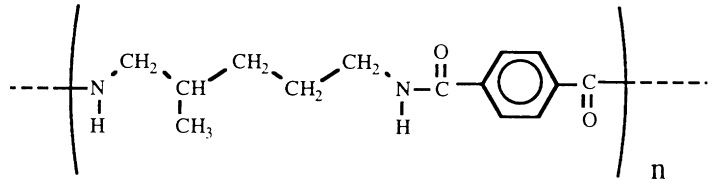

This set of samples allows independent investigation of the role of the different composition parameters (i.e. the tere- or iso-phthalic nature of the aromatic moiety, lactam-12 or methylpentane chemical nature of the aliphatic sequence and lactam-12 amount) that determine the chemical structure of the polymers under study.

2. Experimental

The xT_yI_{1-y} and MT samples were kindly provided by Elf Atochem and Rhône-Poulenc companies, respectively. Their chemical formulae and code names are given in Fig. 1. Their compositions in terms of x and y values, molecular

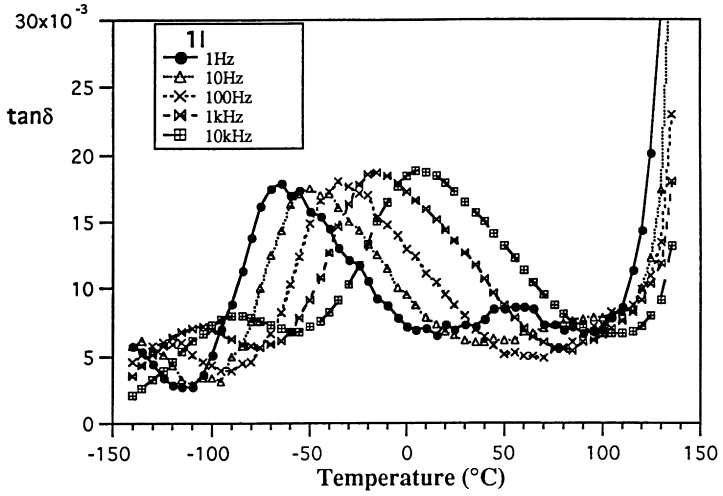

Fig. 2. Dielectric loss tangent vs temperature for 1I at different frequencies.

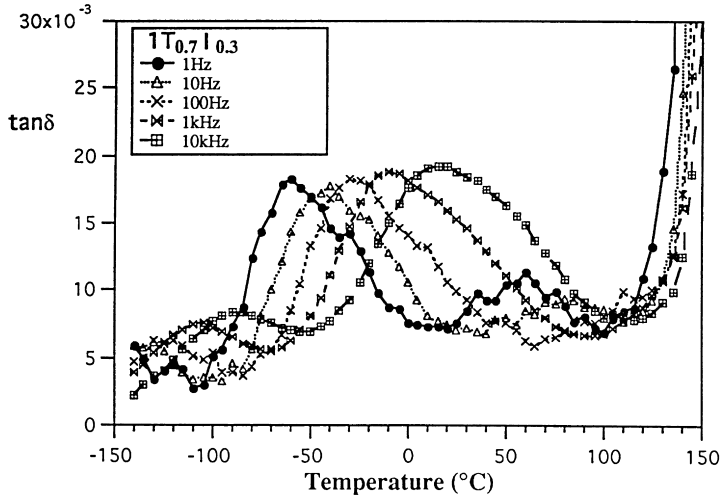

Fig. 3. Dielectric loss tangent vs temperature for $1T_{0.7}I_{0.3}$ at different frequencies.

weight, M_w, amorphous or semicrystalline character, and glass transition temperatures, T_g, are summarized in Table 1. The glass transition temperatures were determined by using a differential scanning calorimeter (DSC) (Du Pont 1090) operating at 10 K min^{-1}. They were estimated from the intersection between the initial base line and the sloping portion of the base line attributable to the glass transition phenomenon. The polymer densities were determined by the flotation method.

Thick films (80–150 μm) were prepared by compression molding under vacuum at $T_g + 50°$ for the amorphous 1I, $1T_{0.7}I_{0.3}$ and 1.8T samples and 320 and 300°C for 1T and MT, respectively. All the samples were carefully annealed under vacuum at $T_g + 20°$ for at least 2 days to remove the residual water. The absence of water was checked by thermal gravimetric analysis that did not detect any loss weight at temperatures below the degradation temperature of 450°C in the annealed films.

Measurements of the complex dielectric function were made in the frequency range $1–10^5$ Hz using a frequency response analyzer (Solartron-Schlumberger FRA 1260 with a Kistler amplifier). A thin (~30 nm) aluminum layer was deposited under vacuum on the polymer films. A square mask, on each side of the polymer film, defined the electrode surface (1 cm^2). The temperature was controlled by a nitrogen gas heating system. The measurements covered a temperature range from −140 to 150°C in 5° steps. No conductivity contribution was detected under the above experimental conditions.

Determinations of the dielectric strength were performed according to the method outlined in Ref. [5]. The

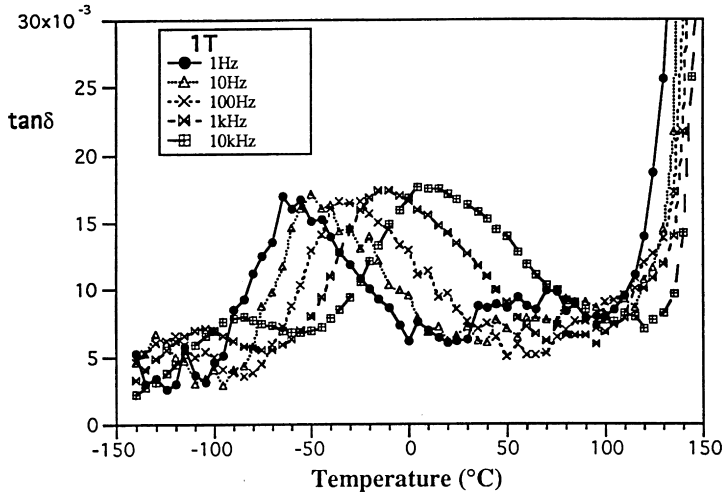

Fig. 4. Dielectric loss tangent vs temperature for 1T at different frequencies.

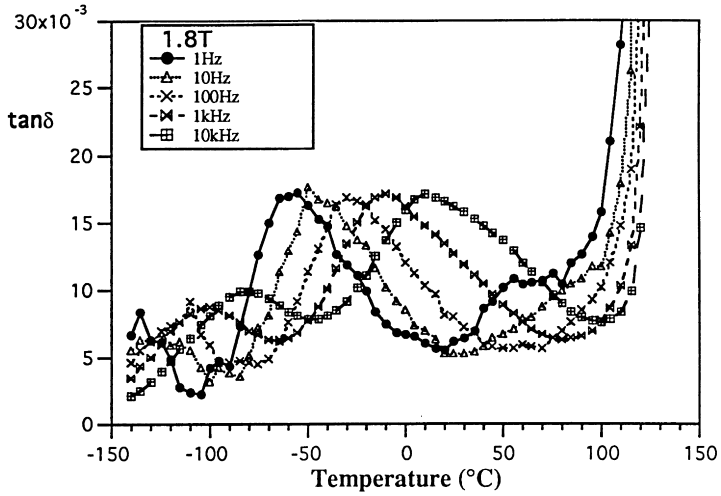

Fig. 5. Dielectric loss tangent vs temperature for 1.8T at different frequencies.

temperatures at the start and end of the β relaxation were measured on the ε'' trace at 1 Hz, which leads to the best resolution of the transitions. The unrelaxed and relaxed ε_u and ε_r values were the ε' values determined at these temperatures. The temperature used in the Onsager expression is the temperature at the end of the relaxation.

3. Results and discussion

3.1. xT_yI_{1-y} copolyamides

The dielectric loss tangents, tan δ, of 1I, $1T_{0.7}I_{0.3}$, 1T and 1.8T are plotted as a function of temperature in Figs. 2–5 for five representative frequencies. As shown in these figures a

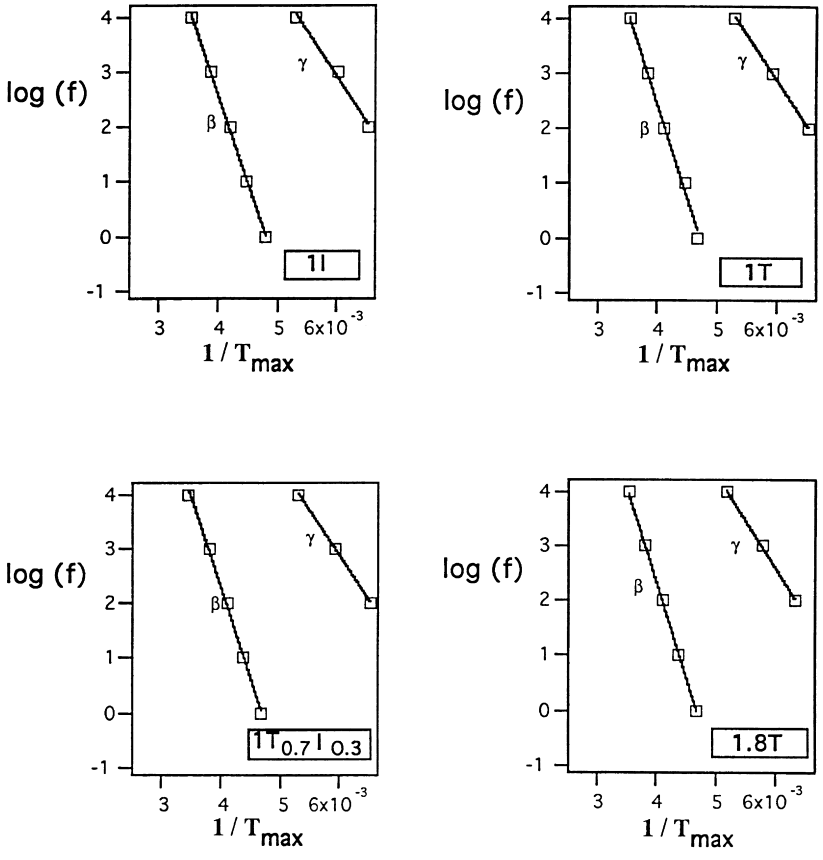

Fig. 6. Dielectric relaxation maps of 1I, $1T_{0.7}I_{0.3}$, 1T and 1.8T.

Table 2
Activation energies and entropies determined for the γ and β relaxations of the different copolyamides

Polyamide	$E_{a\gamma}$ (kJ mol^{-1})	$\Delta S_{a\gamma}$ (J K^{-1} mol^{-1})	$E_{a\beta}$ (kJ mol^{-1})	$\Delta S_{a\beta}$ (J K^{-1} mol^{-1})
1I	31 ± 5	12 ± 35	61 ± 5	56 ± 25
$1T_{0.7}I_{0.3}$	32 ± 5	14 ± 35	63 ± 5	62 ± 25
1T	32 ± 5	15 ± 35	64 ± 5	67 ± 25
1.8T	33 ± 5	18 ± 35	66 ± 5	74 ± 25
MT			57 ± 5	34 ± 25

rapid increase in tan δ is observed at temperatures of the order of 130°C at 1 Hz for 1I, $1T_{0.7}I_{0.3}$ and 1T, and 110°C for 1.8T. This behavior is characteristic for the occurrence of the glass transition phenomenon, which is in good agreement with DSC data reported in Table 1.

At lower temperatures, the dielectric experiments point out the existence of two secondary relaxations: a β transition around −70°C at 1 Hz and a γ transition, with a smaller intensity, which can be seen at high frequencies, for example around −110°C at 1 kHz. At 1 Hz the maximum γ relaxation peak occurs at temperatures below the lowest temperature investigated, i.e. −150°C.

In the temperature range between the glass transition temperature and the β transition, the four samples exhibit a low-intensity broad peak. This additional transition, noted as ω, occurs around 60°C at 1 and 10 Hz. At higher frequencies, it progressively merges with the glass transition phenomenon.

As shown in Figs. 2–5, the γ, β and ω secondary transitions are shifted to higher temperatures on increasing the frequency, f. The frequency dependences of temperatures, T_{max}, at which the maximum of tan δ is observed for β and γ relaxations are plotted in Fig. 6. As indicated by the linear behavior of log(f) as a function of $1/T_{max}$, whatever is the xT_yI_{1-y} polymer considered, the β and γ processes obey an Arrhenius law. The corresponding activation energies, $E_{a\gamma}$ and $E_{a\beta}$, are listed in Table 2, together with the activation entropies, $\Delta S_{a\beta}$ and $\Delta S_{a\gamma}$, calculated according to the Starkweather analysis [6–8]:

$$E_a = RT[1 + \ln(kT/2\pi hf)] + T\Delta S_a \quad (1)$$

within the experimental error, $E_{a\gamma}$ and $E_{a\beta}$ do not depend on the polyamide exact composition.

According to Starkweather [7], low values of the activation entropy can be interpreted in terms of localized motions, whereas higher values (50–100 J K^{-1} mol^{-1}) correspond to cooperative motions. Therefore, the γ transition of copolyamides under study, which has a low activation entropy (10–20 J K^{-1} mol^{-1}), can be assigned to localized motions. The β transition, which has a higher activation entropy (50–80 J K^{-1} mol^{-1}), should correspond to motions with some cooperative character.

3.2. MT copolyamide

The dielectric loss tangent, tan δ, of MT is plotted as a function of the temperature in Fig. 7 for five representative frequencies. As observed in the xT_yI_{1-y} polymers, the rapid increase in tan δ, observed at 1 Hz around 130°C can be assigned to the beginning of the glass transition phenomenon, which is in agreement with the DSC determination of T_g (Table 1). Below T_g, the MT behavior exhibits several differences with respect to the results observed in xT_yI_{1-y} polyamides: the first difference comes from the absence of a transition in the low-temperature region, where the γ transition of xT_yI_{1-y} polymers is observed, even in the

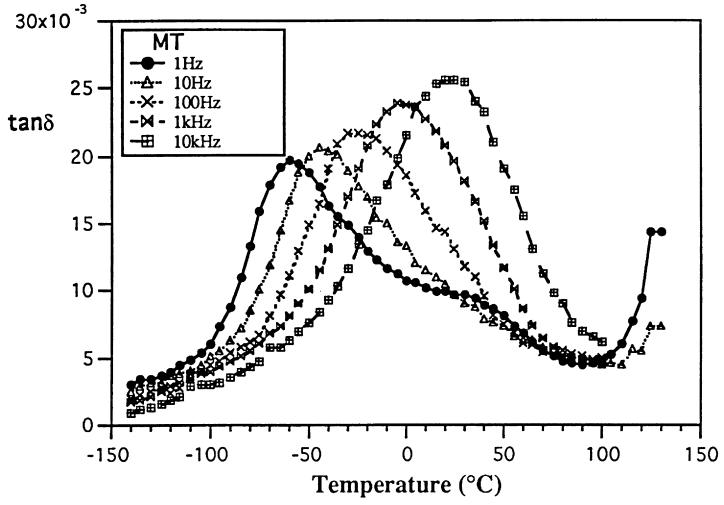

Fig. 7. Dielectric loss tangent vs temperature for MT at different frequencies.

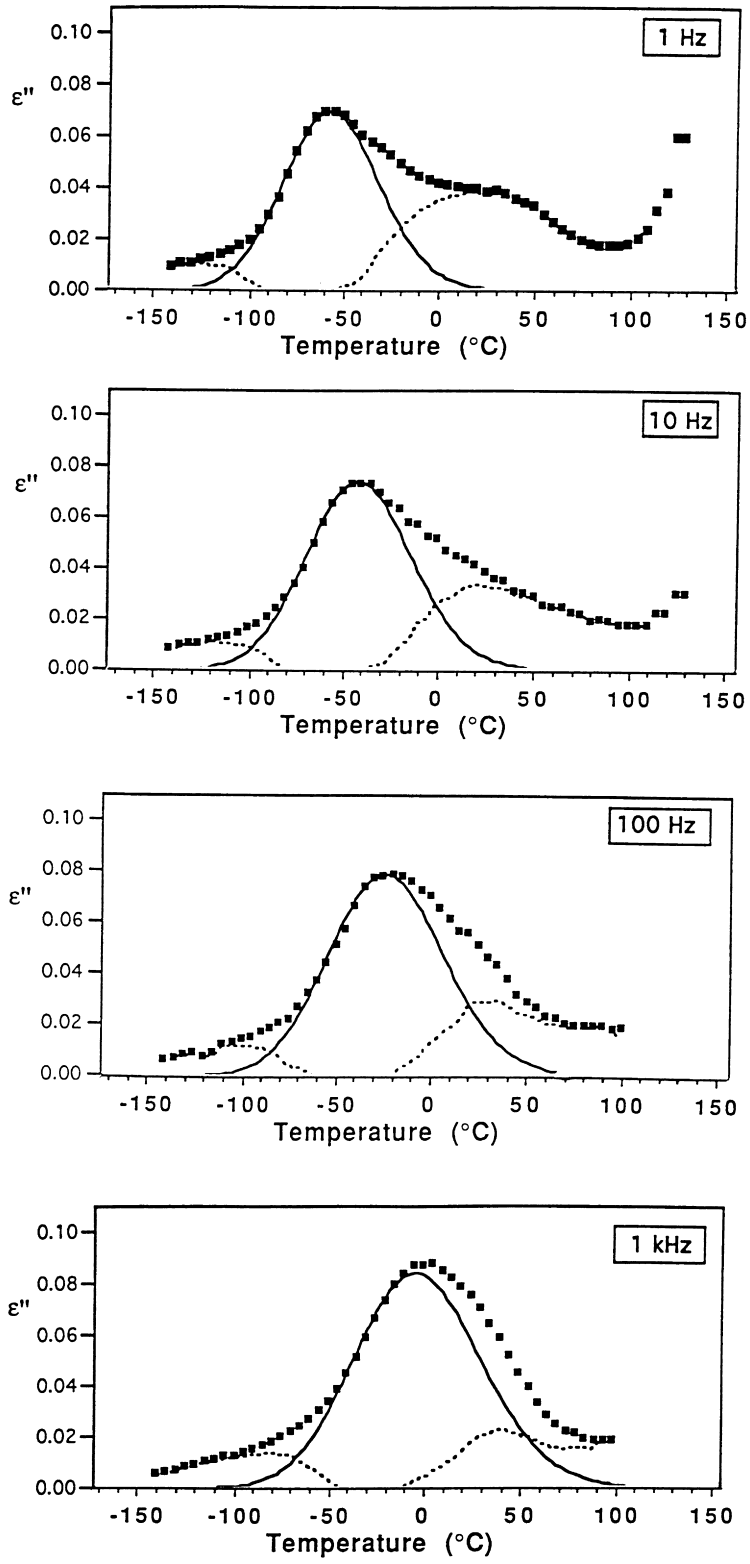

Fig. 8. Dielectric loss ε'' vs temperature obtained at different frequencies for MT: (■), experimental data; (—), calculated β peak using expressions (8) and (9) with the following set of parameters: $\varepsilon_r - \varepsilon_u = 0.47$, $E_a^{ave} = 62.0$ kJ mol^{-1}, $B_2 = 9.9$ kJ mol^{-1}, $\tau_0 = 10^{-16}$ s; (- - -), difference trace.

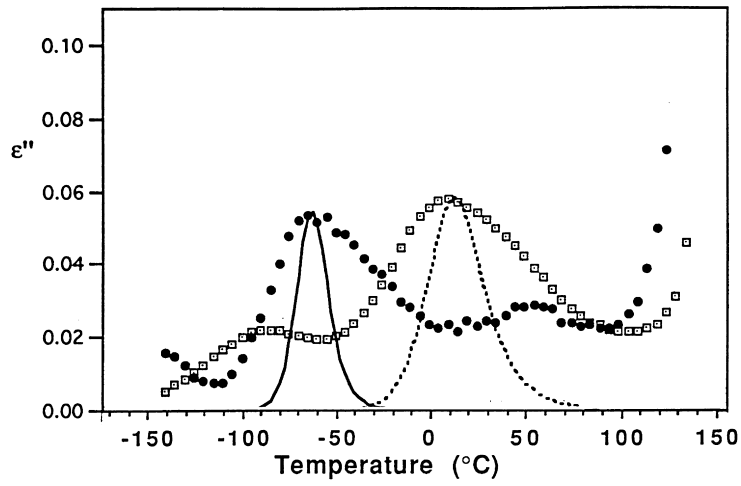

Fig. 9. Dielectric losses ε'' vs temperature obtained for 1I at 1 Hz and 10 kHz.(●): (□), experimental data; (—), (- - -), calculated β peaks using expressions (8) and (9) with the following set of parameters: $\varepsilon_r - \varepsilon_u = 0.13$, $E_a^{ave} = 60.6$ kJ mol^{-1}, $B_2 = 1.7$ kJ mol^{-1}, $\tau_0 = 1.38 \times 10^{-16}$ s.

experiments performed at high frequencies. The second point concerns the characteristics of the broad secondary transition lying in the temperature range from −100 to +80°C. On increasing the frequency, the maximum of the peak is shifted to a higher temperature, the peak intensity increases and the lineshape is modified. At 1 Hz, at least two distinct contributions, can be distinguished in this broad line. The low-temperature part corresponds to a peak centered around −60°C, comparable to the β peak observed at 1 Hz in the xT_yI_{1-y} samples. This contribution will be denoted as β in henceforth. The high-temperature part exhibits a broad shoulder in the temperature range from 0 to 50°C. Curiously enough, the latter contribution is not clearly observed in the dielectric traces recorded at higher frequencies, in disagreement with the expected shift towards high temperature which is characteristic of an Arrhenius behavior. In this regard this second contribution is noticeably different from the ω transition of xT_yI_{1-y} samples.

In order to perform a more detailed analysis of both the low- and high-temperature contributions, we have first looked for a precise description of the β peak at each frequency. The simplest model that can account for the secondary relaxation phenomena is based on a single correlation time τ. Under this assumption, the real and imaginary parts of the permittivity are given by the following Debye expressions [9]:

$$\varepsilon' = \varepsilon_u + \frac{(\varepsilon_r - \varepsilon_u)}{1 + \omega^2\tau^2} \tag{2}$$

$$\varepsilon'' = (\varepsilon_r - \varepsilon_u)\frac{\omega\tau}{1 + \omega^2\tau^2} \tag{3}$$

where ε_r and ε_u are the relaxed and unrelaxed ε' values recorded before and after the transition, respectively. Some dielectric or mechanical transitions can be represented by these simple equations. However, this model does not account for most of the data. When considering a distribution of correlation times, $\psi(\ln\tau)$, ε' and ε'' can be written as [9]:

$$\varepsilon' = \varepsilon_u + (\varepsilon_r - \varepsilon_u)\int_{-\infty}^{+\infty} \frac{\psi(\ln\tau)}{1 + \omega^2\tau^2}\,d(\ln\tau) \tag{4}$$

$$\varepsilon'' = (\varepsilon_r - \varepsilon_u)\int_{-\infty}^{+\infty} \frac{\psi(\ln\tau)\omega\tau}{1 + \omega^2\tau^2}\,d(\ln\tau) \tag{5}$$

A Gaussian distribution is often used [10–12] as follows:

$$\psi(\ln\tau) = \frac{1}{B\sqrt{\pi}}\exp\left[-\left(\frac{\ln\tau - \ln\tau_{ave}}{B}\right)^2\right] \tag{6}$$

where B is the distribution width. Such a function permits to elucidate the origin of the distribution of correlation times. Indeed, using an Arrhenius expression for the correlation time, τ [12]:

$$\tau = \tau_0 \exp\left[\frac{E_a}{RT}\right] \tag{7}$$

it appears that the distribution of τ may originate either from a preexponential factor, τ_0, or from an activation energy, E_a, distribution. Three different possibilities can be considered:

1. a τ_0 distribution only—then, $\psi(\ln\tau)$ corresponds to a $\psi_1(\ln\tau_0)$ Gaussian function with width $B_1 = B$;
2. an E_a distribution only—then $\psi(\ln\tau)$ corresponds to a $\psi_2(E_a)$ Gaussian function with width $B_2 = BRT$;
3. both τ_0 and E_a distributions.

With the assumption of an E_a distribution only, the β peak of MT can be calculated using the following expression:

$$\varepsilon'' = (\varepsilon_r - \varepsilon_u)\int_{-\infty}^{+\infty} \psi_2(E_a)\frac{\omega\tau(E_a)}{1 + \omega^2\tau(E_a)^2}\,d(E_a) \tag{8}$$

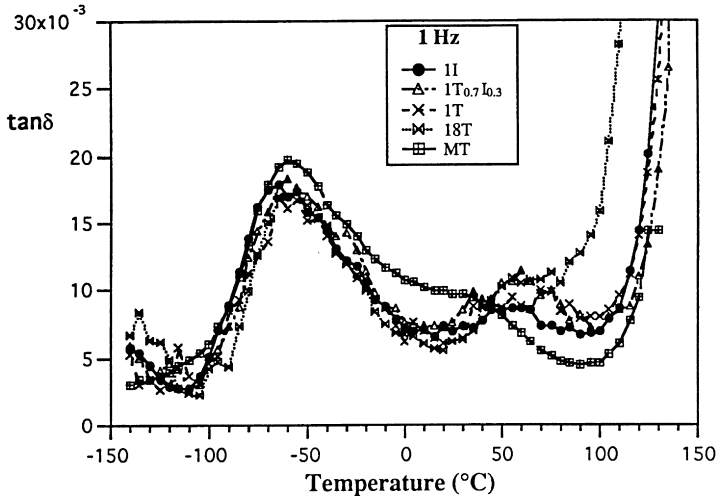

Fig. 10. Dielectric loss tangent vs temperature determined at 1 Hz for the different samples.

with

$$\psi_2(E_a) = \frac{1}{B_2\sqrt{\pi}}\exp\left[-\left(\frac{E_a - E_a^{ave}}{B_2}\right)^2\right] \quad (9)$$

$$\omega = 2\pi f \quad (10)$$

$$\tau(E_a) = \tau_0 \exp\left[\frac{E_a}{RT}\right] \quad (11)$$

The best fit at 1 Hz was obtained by using the following set of parameters: $\varepsilon_r - \varepsilon_u = 0.47$, $E_a^{ave} = 62.0$ kJ mol^{-1}, $B_2 = 9.9$ kJ mol^{-1}, $\tau_0 = 10^{-16}$ s. The β peak was calculated at the different frequencies using these parameters. It was then subtracted from the experimental pattern observed at the same frequency. Results thus obtained are shown in Fig. 8. At each frequency, the calculated β peak is in good agreement with experimental data. The maximum of the peak is located at the same temperature; the width and intensity of the calculated curve are systematically smaller than the experimental ones. Under these conditions, the difference between the calculated β peak and the experimental trace points out the existence of an additional contribution at each frequency that is observed in the same temperature range irrespective of the frequency. Therefore, this additional contribution corresponds to a frequency-independent process.

However, the above assumptions may not be entirely satisfying in the case of the MT polyamide. Indeed, the calculation used to represent the β peak is based on a rather broad ($B_2 = 9.9$ kJ mol^{-1}) distribution of activation energies. However, in all the xT_yI_{1-y} samples investigated, for which the β transition is clearly separated from the other transitions, the intensity of the β peak exhibits only a weak frequency dependence that implies that the activation energy of the β process has quite a narrow distribution. For example, in 1I (Fig. 9) a B_2 width of 1.7 kJ mol^{-1} is sufficient to account for the intensity increase on increasing the frequency. However, as shown in Fig. 9, such a distribution does not describe the width of the experimental β peak. Therefore, a τ_0 distribution must also be considered. In such a case, the different motional modes may not be solicited with the same efficiency at each frequency and the τ_0 distribution may depend on the experimental frequency. In such a case, the calculation of the β peak is no more simple and we have thus preferred the following approach.

Fig.10 shows the comparison of the dielectric loss tangents, tan δ, determined at 1 Hz for the xT_yI_{1-y} and MT samples as a function of the temperature. All the xT_yI_{1-y} polymers exhibit the same β peak within the experimental error. Moreover, the β peak of the MT polyamide is identical to the β peak of xT_yI_{1-y} polymers in the low-temperature range, where the high-temperature contribution does not interfere. Therefore, as a first approximation, the β peak of MT can be described by the β peak of the xT_yI_{1-y} series. Results obtained by subtracting the β peak (after a 1.3 multiplication accounting for the observed intensity) of xT_yI_{1-y} polymers from the experimental dielectric loss tangent of MT are shown in Fig. 11. They point out the existence of an additional contribution that does not depend on the frequency.

As discussed above, the correlation time distribution involved in the β transition of xT_yI_{1-y} polymers is mainly due to a τ_0 distribution rather than to a distribution of activation energies, the nature of the correlation time distribution is not elucidated in MT. The two decompositions performed in this work allow investigation of the two possible origins of the correlation time distribution, i.e. either a distribution of activation energies or a τ_0 distribution. They both lead to the same conclusion: the additional contribution to the β peak observed at high temperature is frequency-independent. It can thus be assigned to a quasi-melting phenomenon. In principle, such a process could be detected by DSC. Fig. 12 shows the DSC trace of MT, recorded at a

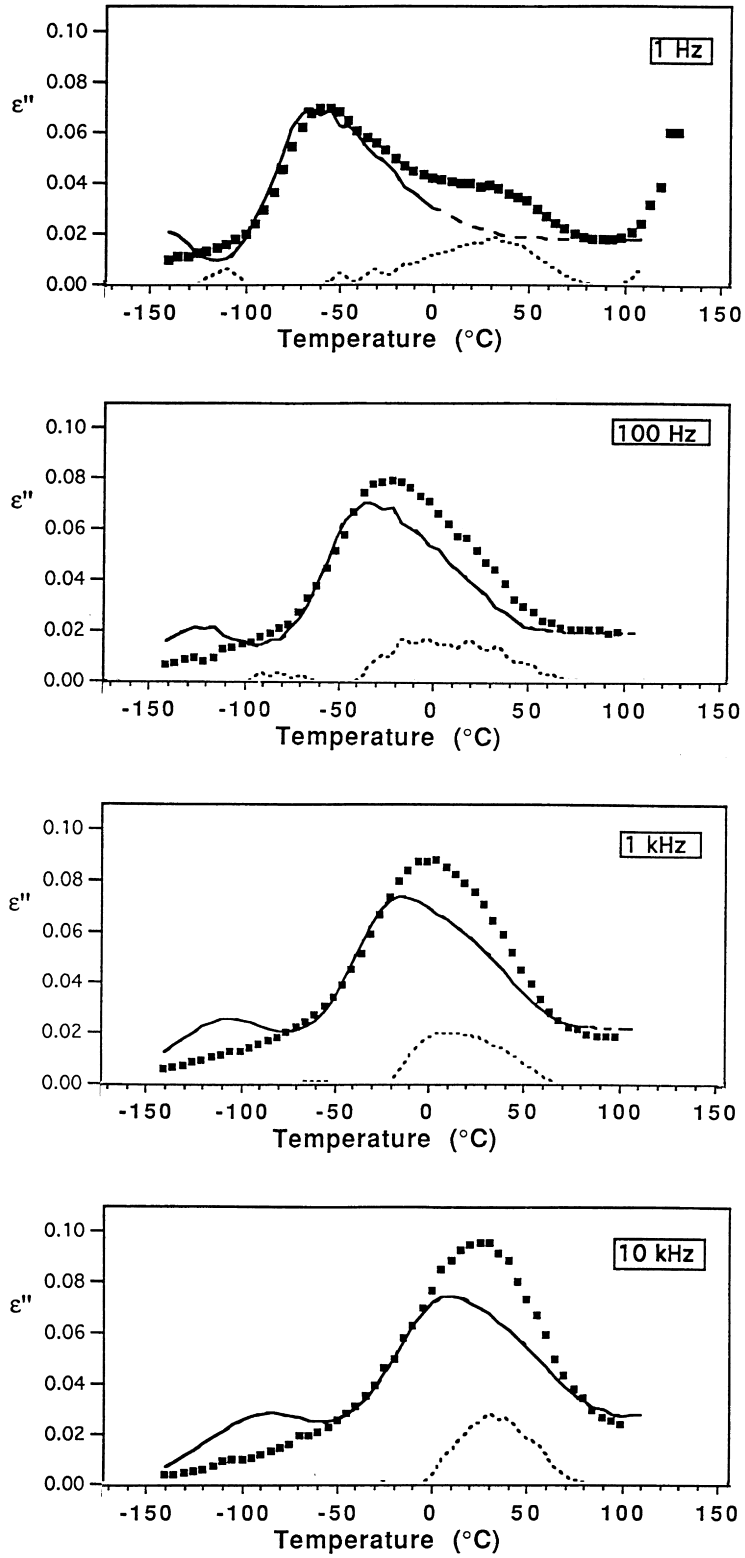

Fig. 11. Dielectric loss ϵ'' vs temperature obtained for MT at different frequencies: (■), experimental data; (—), 1I β peak lineshape; (- - -), difference trace.

$10^{\circ}\,min^{-1}$ heating rate. A change in the slope is observed around 30°C. It indicates the onset of an endothermic event whose maximum is around 80°C. These temperatures are the temperatures at which the maximum and end, respectively, of the quasi-melting process are observed on the difference dielectric traces (Figs. 8 and 11).

The relaxation map of MT is plotted in Fig. 13. The β transition obeys an Arrhenius law. Its activation energy and

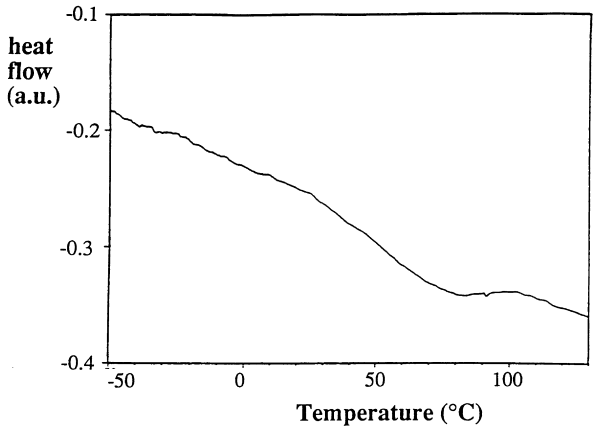

Fig. 12. DSC trace of MT.

entropy are listed in Table 2. The activation energy, $E_{a\beta}$, is very similar to the activation energy determined in xT_yI_{1-y} polymers for the β transition. On the contrary, the activation entropy determined according to Starkweather analysis is quite low, indicating that the β transition of MT is less cooperative than the β transition of xT_yI_{1-y} polymers.

3.3. Assignment of the relaxations

In the copolyamides under study, the dipoles that are responsible for the dielectric relaxations are associated with the C=O groups of the amide functions. Due to the quasi-conjugated character of the CO–NH bond, the amide group takes on a rigid plane conformation and motions about the CO–NH bond are very unlikely [13,14]. Therefore, the dielectric relaxations of polyamides should correspond to motional modes that involve the whole amide groups and not only the carbonyls.

As shown in Fig. 1, depending on their degree of conjugation with the neighboring groups and on the rather rigid or flexible character of these neighbors, three different C=O groups can be distinguished:

1. CO_{aliph} groups that are non-conjugated carbonyl groups situated between two aliphatic units, a flexible lactam-12 unit on one side and a rigid cycloaliphatic unit on the other side. In addition, the 1.8T polyamide also possesses a C=O group, noted CO_{aliph2}, located between two lactam-12 segments.
2. CO_{arom1} groups, which are located between a flexible lactam-12 or methylpentane unit and a phenyl, ring and share some conjugation with the phenyl ring.
3. CO_{arom2} groups, which are located between a rigid cycloaliphatic unit and a phenyl ring and share some conjugation with the phenyl ring.

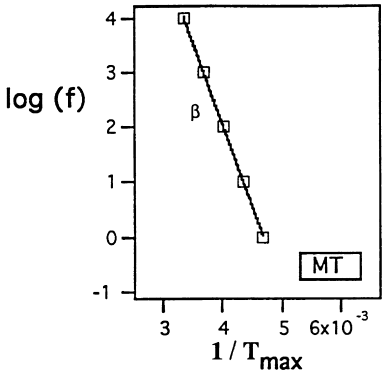

Fig. 13. Dielectric relaxation map of MT.

Regarding the dielectric behavior, the simplest compound is the MT polymer. It contains CO_{arom1} carbonyl groups only. As its dielectric trace exhibits only one transition, this β transition can be unambiguously assigned to the motion of these CO_{arom1} dipoles. This conclusion is markedly different from the results derived for the β transition of aliphatic polyamides. In humid aliphatic polyamides, the β transition is mainly due to amide groups that are hydrogen-bonded to water molecules [9]. In carefully dried aliphatic polyamides, the amide groups that are responsible for the β relaxation are not hydrogen-bonded to other chains. They may belong to short chains or chain ends [9,15,16].

The dielectric traces of 1I, $1T_{0.7}I_{0.3}$ and 1T show a β transition whose characteristics in terms of temperature and activation energy are very close to those of MT (Fig. 10). Therefore, it can be assigned to the CO_{arom1} motions too. These materials exhibit two other transitions, γ and ω, which occur in very different temperature ranges. The two kinds of carbonyl groups, which are not assigned yet, are quite different: the CO_{arom2} group is conjugated with the phenyl ring, whereas the CO_{aliph} is not. The existence of some conjugation implies that the correlation between the CO_{arom2} group and phenyl group is much stronger than the correlation between the CO_{aliph} and its aliphatic environment. In addition, due to the proximity of the flexible lactam-12 unit, the CO_{aliph} groups should exhibit a higher mobility and their motions should occur at lower temperatures than the CO_{arom2} motions. The γ and ω transitions can thus be assigned to the motions of CO_{aliph} and CO_{arom2} carbonyls, respectively.

It must be noticed that both β and ω transitions arise from motions of conjugated carbonyls. The difference in their onset temperature results from the chemical nature of their aliphatic environment. The relaxation of the Co_{arom1} groups, which are next to a lactam-12 unit, more flexible than the cycloaliphatic part, occurs at a lower temperature than the CO_{arom2} transition.

The dielectric behavior of 1.8T in the regions of β and ω transitions is very similar to the behavior observed for the $1T_yI_{1-y}$ polymers, and, therefore, the assignment of these two transitions to motions of the CO_{arom1} and CO_{arom2} groups, respectively, is straightforward. As shown in Figs. 10 and 14, which compare the dielectric behaviors of various samples at 1 Hz and 1 kHz, respectively, there are some differences in the region of the γ transition. It must be

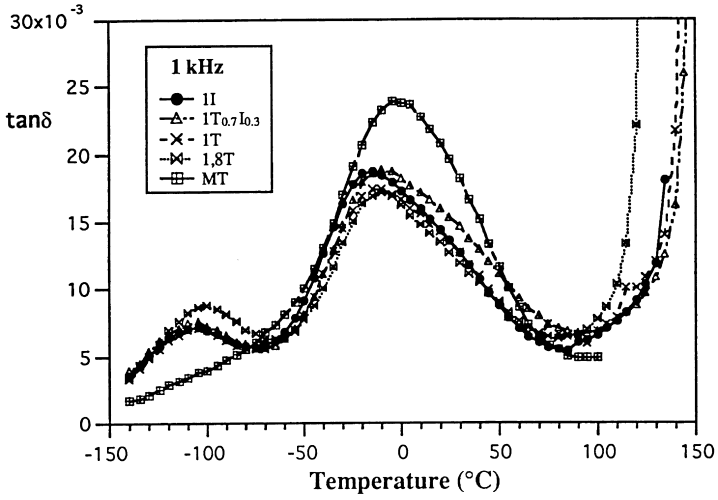

Fig. 14. Dielectric loss tangent vs temperature determined at 1 kHz for the different samples.

noticed that 1.8T possesses two kinds of aliphatic carbonyl groups: in addition to the CO_{aliph} groups, situated between a lactam-12 sequence and cycloaliphatic ring, similar to those found in $1T_yI_{1-y}$ polymers, there are also CO_{aliph2} groups located between two lactam-12 sequences, which benefit from a more flexible environment than the CO_{aliph} groups. Therefore one might be expected to observe two γ relaxations in 1.8T, one being identical to the γ transition of $1T_yI_{1-y}$ polyamides and the other one at a lower temperature, arising from the more mobile CO_{aliph2} groups. However, only one γ relaxation is observed for 1.8T as shown in Figs. 10 and 14. At 1 Hz (Fig. 10), the only difference with the $1T_yI_{1-y}$ samples comes from a higher intensity of γ relaxation. At 1 kHz (Fig. 14), the γ transition of 1.8T is not only more intense than the γ transition of $1T_yI_{1-y}$ samples, but it is also more spread out towards the high-temperature side whereas the onset of the transition, in the low-temperature part, is unchanged. This result shows the existence of an additional contribution, denoted γ′, occurring at a higher temperature than the CO_{aliph} process of $1T_yI_{1-y}$ polymers. This γ′ contribution, centered around −92°C, is clearly shown in the 1 kHz difference trace plotted in Fig. 15 with the 1I sample being taken as reference. The same decomposition, performed at 100 Hz and 10 kHz, leads to the determination of a 42 kJ mol^{-1} activation energy and a 59 J K^{-1} mol^{-1} activation entropy. The latter value is significantly higher than the 12–15 J K^{-1} mol^{-1} $\Delta S_{a\gamma}$ value derived for the $1T_yI_{1-y}$ polyamides. As compared with the CO_{aliph} motional process observed in the $1T_yI_{1-y}$ polymers, it indicates a more cooperative character for motions responsible for the γ′ contribution. Therefore, the increase in flexibility associated with the larger amount of lactam-12 units is compensated by a larger cooperativity.

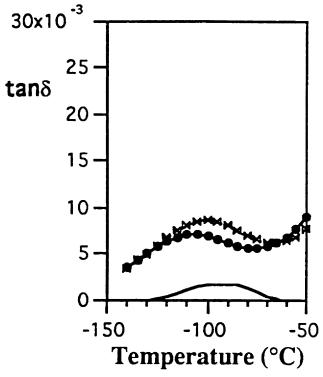

Fig. 15. Dielectric loss tangent vs temperature determined at 1 kHz for 1.8T (×) and 1I (●); (—): difference trace.

In aliphatic polyamides, the γ dielectric transition is systematically associated with a γ mechanical transition, assigned to motions of the $(CH_2)_n$ sequences [9,17–19]. As will be shown in a forthcoming paper [1], these $(CH_2)_n$ sequences are also likely to be involved in the γ transition of aryl–aliphatic copolyamides. The activation energies derived for the γ process in polyamide 12 (28.1 kJ mol^{-1}) [20] and polyamides 3 and 4 (33.4 kJ mol^{-1}) [21] are in good agreement with the activation energy calculated for the γ process in the present work (31–33 kJ mol^{-1}). On the contrary, the temperatures at which the maximum of the γ dielectric transition is observed at 1 Hz on several aliphatic polyamides [20] (Table 3) are higher than those observed for xT_yI_{1-y} polymers. They are quite close to the temperature (−92°C) corresponding to the maximum of the high-temperature γ′ contribution occurring in 1.8T. This result

Table 3
Temperatures at which the maximum of the γ dielectric transition is observed at 1 Hz on several aliphatic polyamides [20]

Polyamide	PA-6	PA-6,6	PA-6,10	PA-12
Temperature (°C)	−73	−96	−97	−78

Table 4
Areas (%) under the β and γ transitions and efficiency factors determined at 1 kHz

Polyamide	γ area (%)	β area (%)	(e_β/e_γ)
1I	16.0	84.0	5.25
$1T_{0.7}I_{0.3}$	16.1	83.9	5.21
1T	16.2	83.8	5.17
1.8T	21.7	78.3	

is consistent with the fact that CO_{aliph2} groups, just as C=O groups of aliphatic polyamides, are situated between two flexible $(CH_2)_n$ sequences. Therefore, in the present work, the low-temperature part of the γ peak, observed in all xT_yI_{1-y} samples under study, can be assigned to CO_{aliph} modes possibly enhanced by the methylene motions of the flexible sequence. The high-temperature γ′ contribution in 1.8T is assigned to CO_{aliph2} motional processes with a spatial scale larger than the CO_{aliph} ones, involving not only the aliphatic carbonyl groups located between two lactam-12 units but also the adjacent methylene units on both sides.

3.4. Influence of the proportion of lactam-12 sequences and positions of the substituents on the aromatic rings

The areas under the transitions, defined by the ε'' dependences, are directly related to the dissipated energy [9]. Contrary to tan δ, ε'' is sensitive to eventual changes in the film thickness. However, this error can be corrected by normalizing the area under each transition by the sum of the areas under the γ and β processes. As shown in Table 4, the γ transition accounts for 16–16.2% of the total area in $1T_yI_{1-y}$ polymers. In 1.8T, the γ and γ′ transitions contribute to 21.7% of the total area.

The relevant parameter is the dipole density

$$N_i = X_i d \frac{N_{Av}}{M} \tag{12}$$

where N_i is the density of a given dipole i, X_i the number of dipoles i per repeat unit, d the polymer density, N_{Av} the Avogadro constant and M the molecular weight of the repeat unit. Results listed in Table 5 show that the CO_{aliph} density is constant in $1T_yI_{1-y}$ series, as well as the relative area below the γ transition (16–16.2%).

The relative area under a given relaxation i can be written as the product of the corresponding dipole density, N_i, by an efficiency factor, e_i:

$$\%\gamma \text{ area} = \frac{N_\gamma e_\gamma}{N_\gamma e_\gamma + N_\beta e_\beta} = \frac{N_\gamma}{N_\gamma + N_\beta \dfrac{e_\beta}{e_\gamma}} \tag{13}$$

$$\%\beta \text{ area} = \frac{N_\beta e_\beta}{N_\beta e_\beta + N_\gamma e_\gamma} = \frac{N_\beta}{N_\beta + N_\gamma \dfrac{e_\gamma}{e_\beta}} \tag{14}$$

The e_β/e_γ ratios, determined from areas under transitions, are given in Table 4 for $1T_yI_{1-y}$ polymers. They do not vary in $1T_yI_{1-y}$ series. As, in all these materials, the CO_{aliph} groups have the same environment, and, therefore, the same motions and e_γ factor, this result indicates that the e_β factor describing the efficiency of the CO_{arom1} motions is also a constant in this series. It thus appears that the relative, *meta* or *para*, positions of the substituents on the phthalic moiety have no detectable influence on the dielectric relaxation of the CO_{arom1} units. This conclusion implies that either the motions of CO_{arom1} groups and phenyl rings are uncorrelated or the local dynamics of the phenyl rings is independent of the position of the substituents. This question will be addressed in a forthcoming paper using high-resolution solid-state ^{13}C NMR experiments [1].

By using an efficiency ratio e_β/e_γ of 5.20, taken from results listed in Table 4, one can calculate relative areas of 25.7 and 74.3% below the γ + γ′ and β transitions, respectively, in 1.8T. These values are in reasonable agreement with the experimental results determined from dielectric traces at 1 kHz, i.e.: 21.7 and 78.3%, respectively. Therefore, within an experimental error, the γ + γ′ contribution in 1.8T appears to be characterized by the same e_γ factor that governs the γ relaxation of $1T_yI_{1-y}$ polymers.

More information on the β relaxation can be obtained by considering the dielectric relaxation strength $\Delta\varepsilon$, which corresponds to the area below the dielectric loss curves measured for the transition. Its expression is given by the Onsager equation

$$\Delta\varepsilon = \frac{\varepsilon_r(\varepsilon_u + 2)^2}{2\varepsilon_r + \varepsilon_u} \frac{4\pi N\mu^2}{9kT} \tag{15}$$

where N denotes the number of monomeric units per unit volume and μ the dipole moment per monomer unit.

This expression, that derives the strength of a dielectric relaxation arising from dipoles that are freely rotating about the chain local axis, was initially used for the glass transition phenomenon. It was then applied to secondary transitions

Table 5
Density and dipole densities for the different samples

Polyamide	Density (g cm^{-3})	$X_{CO_{aliph}}$	$10^{27} \times N_{CO_{aliph}}$ (dip m^{-3})	$X_{CO_{arom1}}$	$10^{27} \times N_{CO_{arom1}}$ (dip m^{-3})
1I	1.055	1	1.125	1	1.125
$1T_{0.7}I_{0.3}$	1.057	1	1.127	1	1.127
1T	1.054	1	1.124	1	1.124
1.8T	1.042	1.8	1.563	1	0.868

Table 6
Experimental and calculated dielectric strength, $\Delta\varepsilon$, of the β relaxation, using the Onsager expression, $\mu = 2.4D$ and $D = 3.33564 \times 10^{-30}$

Polyamide	ϵ_u	ϵ_r	Experimental $\Delta\varepsilon$	Calculated $\Delta\varepsilon$
1I	2.802	3.304	0.502	1.842
$1T_{0.7}I_{0.3}$	2.970	3.494	0.524	2.009
1T	2.981	3.486	0.505	1.941
1.8T	2.878	3.359	0.481	1.438

[5,22,23]. Results obtained according to Ref. [5] by assuming that all the CO_{arom1} dipoles are freely rotating are listed in Table 6. They show that the measured dielectric strength is always lower than the calculated one. This difference may be due to the fact that only a fraction of CO_{arom1} dipoles are flipping. The ratio of the experimental dielectric strength to the calculated one is of the order of 0.3, independent of the xT_yI_{1-y} polymer investigated. This result is consistent with the fact that the β relaxation exhibits the same efficiency factor in all these samples.

4. Conclusion

Dielectric relaxation measurements performed on five aryl–aliphatic copolyamides have shown two different behaviors: xT_yI_{1-y} polymers exhibit three secondary relaxations denoted as γ, β and ω with an increasing temperature. On the contrary, MT shows only one secondary transition. This different behavior, as well as the dependence of dielectric data as a function of the chemical composition of samples, has led to the identification of dipoles that are involved in motional processes responsible for these relaxations.

The γ relaxation is due to motions of non-conjugated amide groups. The aliphatic environment of these groups determines the spatial scale of the motions in which they are involved. Amide groups located between a lactam-12 sequence and a cycloaliphatic moiety undergo localized modes characterized by low activation entropy and energy. Amide groups that are between two lactam-12 sequences exhibit motions with a higher activation entropy and, therefore, a higher cooperative character.

β and ω relaxations originate from motions of amide functions that are conjugated with phenyl rings. The 120°C temperature difference that separates these two processes at 1 Hz can be explained in terms of local environments of these functions. Dipoles responsible for the β transition are C=O groups next to a flexible lactam-12 or methylpentane sequence, whereas dipoles responsible for the ω transition are bound to a rigid cycloaliphatic moiety. The β relaxation of the xT_yI_{1-y} polymers has a 60–70 $J\,K^{-1}\,mol^{-1}$ activation entropy that corresponds to motions with some cooperative character.

The ω transition is a very broad, ill-defined transition which could not be studied in detail. In addition to these secondary relaxations, the MT polymer exhibits a frequency-independent phenomenon, located around 30°C. In agreement with the DSC results, it has been assigned to a quasi-melting process.

Acknowledgements

It is a pleasure to acknowledge ELF-ATOCHEM, France for its interest in the study and financial support of one of us (F.B.).

References

[1] Beaume F, Lauprêtre F, Monnerie L. In preparation.
[2] Garin N, Hirschinger J, Beaume F., Lauprêtre F. In preparation.
[3] Beaume F, Brûlé B, Halary JL, Lauprêtre F, Monnerie L. In preparation.
[4] Judas D, Blondel P, Melot D. Personal communication.
[5] Alhaj-Mohammed MH, Davies GR, Abdul-Jawad S, Ward IM. J Polym Sci, B: Polym Phy 1988;26:1751.
[6] Starkweather HW. Macromolecules 1981;14:1277.
[7] Starkweather HW. Macromolecules 1988;21:1798.
[8] Starkweather HW. Polymer 1991;32:2443.
[9] McCrum NG, Read BE, Williams G. Anelastic and dielectric effects in polymeric solids, New York: Wiley, 1967.
[10] Wehrle M, Hellmann GP, Spiess HW. Coll Polym Sci 1987;265:815.
[11] Rössler E, Taupitz M, Börner K, Schultz M, Vieth HM. J Chem Phy. 1990;92:5847.
[12] Montes H. Thèse, Institut National Polytechnique de Grenoble, 1994.
[13] Tsvetkov VN, Shtennikova IN. Macromolecules 1978;11:306.
[14] Lauprêtre F, Monnerie L. Eur Polym J 1978;14:415.
[15] Kolarik J, Janacek J. J Polym Sci, C: Polym Symp 1967;16:441.
[16] LeHuy HM, Rault J. Polymer 1994;35:136.
[17] Starkweather HW, Barkley JR. J Polym Sci, B: Polym Phy 1981;19:1211.
[18] Leung WP, Ho KH, Choy CL. J Polym Sci, B: Polym Phy 1984;22:1173.
[19] Varlet J, Cavaillé J-Y, Perez J. J Polym Sci, B: Polym Phy 1990;28:2691.
[20] Pathmanathan K, Cavaille J-Y, Johari GP. J Polym Sci, B: Polym Phy 1992;30:341.
[21] Wolfe E, Stoll B. Coll Polym Sci 1980;258:300.
[22] Ezquerra TA, Balta-Calleja FJ, Zachmann HG. Acta Polymerica 1993;44:18.
[23] Diaz-Calleja R. Macromol Chem Phy 1995;196:3281.